Kinetics of luminescence decay in electron-irradiated sapphire crystals

1997 J. Phys.: Condens. Matter 9 6457

(http://iopscience.iop.org/0953-8984/9/30/014)

J. Phys.: Condens. Matter **9** (1997) 6457–6465. Printed in the UK PII: S0953-8984(97)81730-4

Kinetics of luminescence decay in electron-irradiated sapphire crystals

Kevin J Caulfield†, Ronald Cooper† and John F Boas‡

† Department of Chemistry, The University of Melbourne, Parkville 3052, Victoria, Australia
‡ Australian Radiation Laboratory, Lower Plenty Road, Yallambie 3085, Victoria, Australia

Received 10 February 1997, in final form 24 April 1997

Abstract. The kinetics of luminescence decay in electron-irradiated sapphire (α-Al_2O_3) single crystals have been investigated using time-resolved luminescence spectroscopy. The data, observed over timescales from tens of nanoseconds to tens of milliseconds, characteristically feature a rapid decay of intensity punctuated by discrete plateau regions. Simple theoretical models, invoking such theories as first- or second-order mechanisms, rate laws or power-law dependences, are unable to explain these features. A theoretical model comprising bimolecular electron–hole recombination, together with unimolecular electron detrapping from two discrete traps, qualitatively accounts for these features.

1. Introduction

Point defects created in single crystals of CaO, MgO and α-Al_2O_3 (sapphire) by electron irradiation give rise to luminescence from colour centres. This luminescence may be used to monitor the formation of point defects by elastic collision processes and to observe the time-dependent spectroscopy of the colour centres [1].

The kinetics of luminescence decay may be studied using pulse radiolysis techniques. Analysis of luminescence decay data files from times in the nanosecond region to longer times in the millisecond region reveals several distinctive features of luminescence kinetics. The data, presented logarithmically, show an initially rapid decrease in intensity followed by discrete plateau regions, and a further rapid decay in intensity. The same general features are commonly observed over comparable timescales in similar systems. Studies by Williams *et al* [2] and Rosenblatt *et al* [3] on thermochemically reduced (TCR) MgO, and by Park *et al* [4] on TCR CaO, show very similar features in the emission kinetics, namely a persistent decay and discrete plateau regions. As yet, however, there is no complete model or description which can adequately describe the physical processes which contribute to the luminescence observed over such wide time domains.

Luminescence decay kinetics are controlled by the trapping, release and recombination of charge carriers. Simple first-order [5] and second-order [6, 7] mechanisms for luminescence are unable to fully describe the phenomena observed experimentally.

Radiative recombination of electrons trapped on donors with holes trapped on acceptors has been applied to luminescence from ZnS and related semiconductors by several researchers [8–10]. Williams *et al* [2] applied a donor–acceptor tunnelling recombination model developed by Thomas *et al* [11] to emission decay data from electron-irradiated MgO. They found that for their decay curves for two different emission bands of MgO,

0953-8984/97/306457+09$19.50

attributed to V centres, the data generally showed a much longer decay than was expected theoretically. This shows that the donor–acceptor tunnelling recombination model alone cannot adequately describe the features of luminescence kinetics in MgO over a wide time domain.

In 1984 Jonscher and de Polignac [12] presented an extensive review of the then-available experimental data on the time dependence of luminescence in solids. In general, for a logarithmic representation of luminescence decay data, a power-law time dependence of intensity ($I \propto t^{-s}$) was observed with exponents (s) in the range from 1 to 2. Similar power laws have been successfully applied to dielectric relaxation [13] and to recombination in semiconductors [14].

Given the apparent wide applicability of power laws to luminescence decay data, Jonscher and de Polignac proposed a physical model [12] in which one set of deep traps feeds a second set, and the second in turn feeds the luminescence process. This system was able to account for some aspects of the observed experimental behaviour and to provide a limited explanation of luminescence in solids.

Rosenblatt *et al* [3] developed an energy level diagram to explain the features of F and F^+ luminescence decay data in TCR MgO. After absorption of a photon, an electron in the F or F^+ excited state may fall into a relaxed excited state from which it will undergo a luminescence transition to the ground state of the F or F^+ centre.

Edel *et al* [15] earlier proposed a similar model for F-centre luminescence. They suggested that F centres themselves could act as electron traps through a postulated metastable state, $F^\dagger$. The similarity between the two models lies in the combination of an ionization and a tunnelling process. The difference is in the proposed identity of the electron trap. Whilst there has been no direct observation of an $F^\dagger$ state, the role of H^- centres as electron traps in TCR MgO is well established [16–18].

A study by Swandic [19] applied a stochastic approach to recombination luminescence with retrapping and continuous irradiation. A master equation was derived for the simple case of a single trapping level and a single recombination centre, and the model can be generalized to the more realistic situation of multiple charge traps and recombination centres.

Hughes [20] and Klaffky *et al* [21] have proposed simple two-trap models to explain the radiation-induced conductivity (RIC) observed in sapphire. These comprise shallow and deep electron traps with a single recombination centre at a hole trap. Hughes [20] studied the transient x-ray-induced conductivity in sapphire, and only two plateau regions were observed in the experimental timescale, indicating that only two of the four postulated release rates were significant at room temperature. Klaffky *et al* [21] studied the steady-state radiation-induced conductivity (RIC) in electron-irradiated sapphire, assuming that electrons are the mobile carriers, and developed a model comprising two electron traps and a single hole trap.

In the present study the kinetics of luminescence decay from electron-irradiated sapphire are presented, and a two-level electron-detrapping model is developed in order to describe the features typically observed in experimental data. In summary the model comprises rapid recombination of free electrons with relatively immobile holes, followed by delayed recombination resulting from fast initial trapping of electrons with subsequent slow thermally activated release.

2. Experimental details

A cylindrical single crystal of sapphire (α-Al_2O_3) of approximate diameter 2.5 mm and length 18 mm was obtained from W and C Spicer Limited (Cheltenham, UK). An impurity

analysis of the crystal was performed by Element Analysis Corporation (Tallahassee, Florida, USA) using proton-induced x-ray emission (PIXE). Of the 72 detectable elements, twelve impurity ions were detected, with the major impurities being several hundred parts per million of silicon, chlorine and calcium [22].

The sapphire crystal was irradiated by an electron accelerator (Febetron 706, Hewlett–Packard, Field Emission Division, McMinnville, Oregon, USA). The Febetron produces single pulses of electrons with a pulse width of approximately 3 ns, a maximum energy of 12 J per pulse, and electron energy selectable within the range 0.20 to 0.60 MeV.

The crystal was mounted in an evacuated irradiation cell attached to the electron accelerator. Luminescence from the crystal was focused, perpendicular to the direction of irradiation, onto the entrance slit of a monochromator (Spex Industries, Minimate 1670) whose output was monitored with a photomultiplier (EMI, 9783B) and displayed on a fast-storage oscilloscope (Tektronix, 7633). Emission intensity–time data were digitized from the oscilloscope after capture by a video camera (Sony, AVC-3250 CE) interfaced to an LSI-11 computer system. Individual data files from successive timescales were sequentially normalized to obtain a single decay curve covering the entire timescale of detectable luminescence.

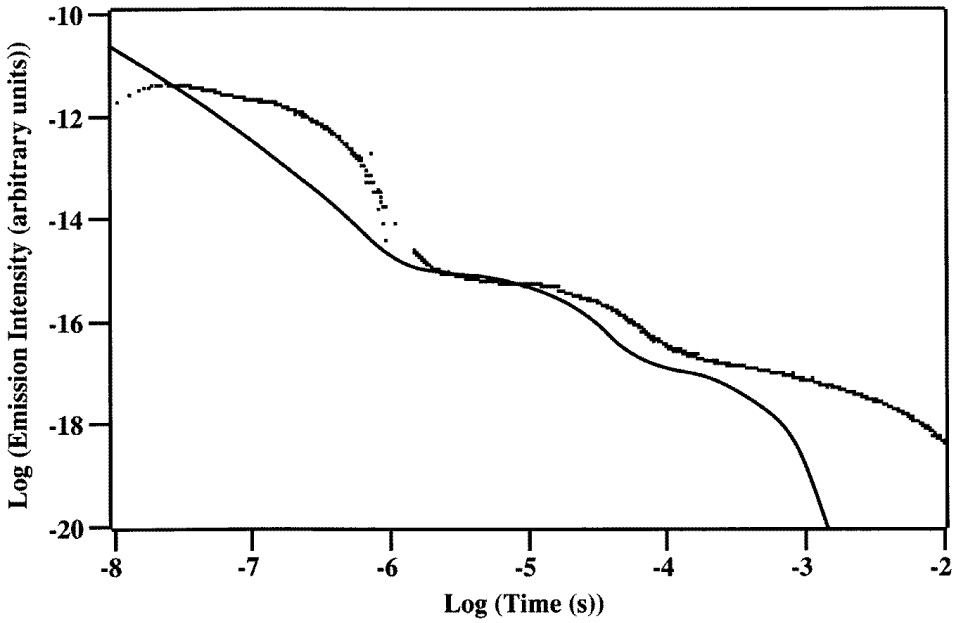

Figure 1. Kinetics of the luminescence decay for 300 nm emission from sapphire irradiated with 0.48 MeV electrons (small squares), compared with the two-level electron-detrapping theory (continuous curve) for the values k_1 to k_4 respectively of 3×10^{14} M^{-1} s^{-1}, 9×10^4 s^{-1}, 5×10^3 s^{-1} and 1×10^{12} s^{-1}, and initial concentrations of $[r] = 1.00 \times 10^{-6}$ M, $[e] = 9.84 \times 10^{-7}$ M, $[e'] = 1.20 \times 10^{-8}$ M and $[e''] = 4.00 \times 10^{-9}$ M.

A two-level electron-detrapping model was developed using 'LARKIN', a FORTRAN computer program which was designed for the numerical simulation of large chemical reaction systems [23]. The program enables the user to monitor the concentrations of species in a reaction system as a function of time.

'LARKIN' uses a stiff integrator to solve a series of differential equations which

represent the reaction system. Initial concentrations are entered and the reaction system is expressed as a series of unimolecular and bimolecular chemical equations with corresponding rate constants.

3. Results

The sapphire single crystal was irradiated with 0.48 MeV electrons (at room temperature), and the luminescence emission monitored at 300 nm. This wavelength corresponds to an emission which we have previously reported [22]. A sample of sapphire from another supplier, Union Carbide, with much higher purity, also produced emission at 300 nm, where F^+ luminescence is expected to occur. We have previously suggested that the 300 nm emission may be due to an F-centre transition proposed by Brewer *et al* [24]. Although the 325 nm F^+ emission was not observed for the Spicer sapphire, it may be underlying the stronger 300 nm band.

Data files were collected for successive timescales for 0.48 MeV electron irradiation at 300 nm, and sequentially normalized to produce a single decay profile. The resulting curve, presented in figure 1, shows the characteristic features of a rapid initial decay, followed by two distinct plateau regions and a final rapid decay.

4. The model

The present reaction system may be expressed as a series of equations, which describe the process of electron–hole recombination, the detrapping of electrons from each of two energy levels, and the luminescence emission arising from radiative recombination.

The model can be expressed as

$$\mathrm{e} + \mathrm{r} \xrightarrow{k_1} \mathrm{P}$$
$$\mathrm{e}' \xrightarrow{k_2} \mathrm{e}$$
$$\mathrm{e}'' \xrightarrow{k_3} \mathrm{e}$$
$$\mathrm{P} \xrightarrow{k_4} h\nu$$

where e is an electron, r is a radiative recombination site, for example an ionized F-type defect centre, P is the product of electron–hole recombination and the precursor of luminescence, e′ is an electron in the shallower trap, e″ is an electron in the deeper trap, $h\nu$ is the luminescence emitted after recombination, and k_1 to k_4 are the rate constants for the various reactions. The trapping of electrons e′ and e″ is considered to be essentially complete by the end of the 3 ns electron beam pulse. In this model, only unimolecular detrapping and bimolecular recombination are considered. No electron or hole tunnelling processes are included.

5. Simulations

Various combinations of initial species concentrations and rate constants k_1 to k_4 were entered into 'LARKIN' to simulate the luminescence decay arising from a two-level electron-detrapping system. Figure 1 shows the resulting simulated decay curve for the rate constant values for k_1 to k_4 respectively of 3×10^{14} M^{-1} s^{-1}, 9×10^4 s^{-1}, 5×10^3 s^{-1} and 1×10^{12} s^{-1}, and initial concentrations of $[r] = 1.00 \times 10^{-6}$ M, $[e] = 0.984 \times 10^{-6}$ M, $[e'] = 0.012 \times 10^{-6}$ M and $[e''] = 0.004 \times 10^{-6}$ M. The processes of electron–hole recombination

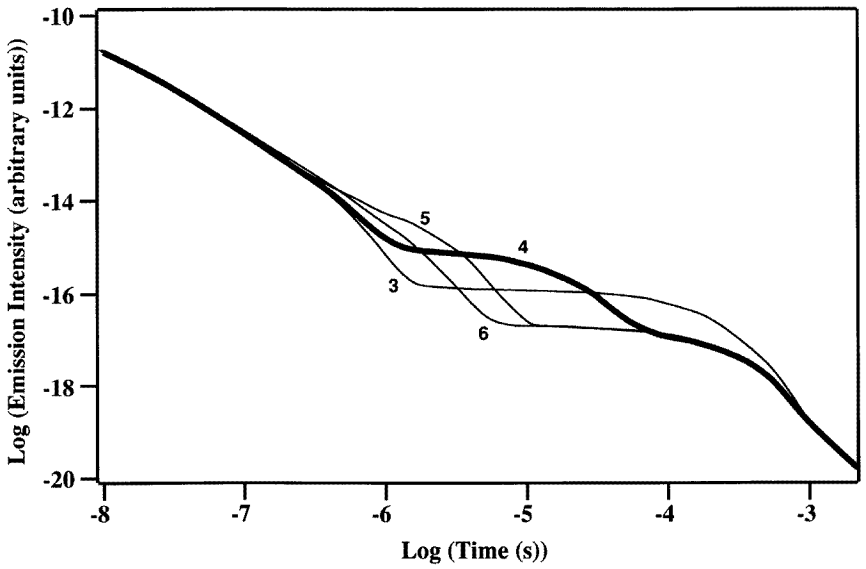

Figure 2. The effect of varying k_2. $k_1 = 3\times10^{14}$ M^{-1} s^{-1}, $k_3 = 5\times10^{3}$ s^{-1}, $k_4 = 1\times10^{12}$ s^{-1}. $k_2 = 9\times10^{n}$ s^{-1}, where the values of n are shown.

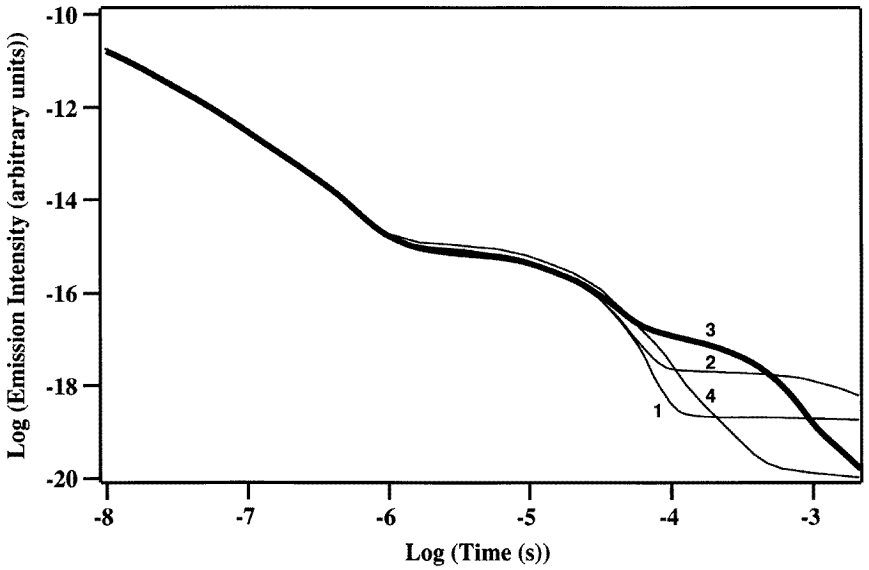

Figure 3. The effect of varying k_3. $k_1 = 3\times10^{14}$ M^{-1} s^{-1}, $k_2 = 9\times10^{4}$ s^{-1}, $k_4 = 1\times10^{12}$ s^{-1}. $k_3 = 5\times10^{n}$ s^{-1}, where the values of n are shown.

and luminescence emission are very rapid, whilst the detrapping processes are comparatively very slow. The defect concentration values used are comparable with literature values of approximately 10^{17} defects per cm^3 for neutron-irradiated sapphire [25] and approximately 10^{16} defects per cm^3 for electron-irradiated sapphire [26]. The experimental data are compared with these simulated data in figure 1. This is not a 'best fit' but a preliminary

attempt to simulate the general features observed in the experimental data, with physically relevant parameters. Using the rate constants and initial concentrations from the simulation in figure 1 as a basis for comparison, the sensitivity of the model to changes in parameters was studied.

The rate constants k_1 to k_4 were varied in order to observe the effects of changes. In each case, the rate constant was twice increased by an order of magnitude (from the values used for the simulation in figure 1) and twice decreased by an order of magnitude, except for the situation in which the rate constant for deep detrapping would become greater than that for shallow detrapping, or the rate constant for shallow detrapping would become less than that for deep detrapping (that is, where k_2 would become less than k_3, or k_3 would become greater than k_2).

Figure 2 shows the effect of varying k_2 whilst figure 3 shows the effect of varying k_3.

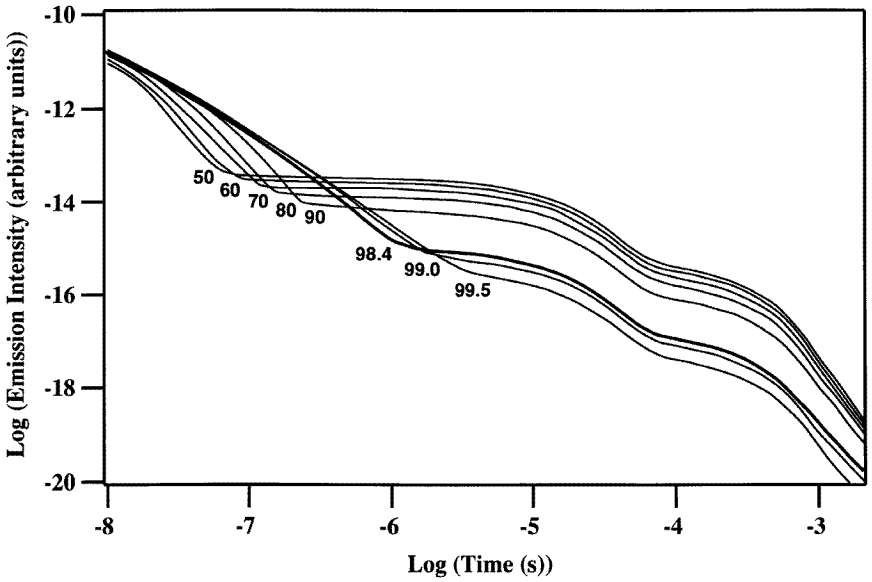

Figure 4. The effect of varying the relative concentrations of free (e) and trapped (e', e'') electrons. The numbers shown represent the percentage of free electrons, with [e']:[e''] a ratio of 3:1 in all cases.

The relative proportions of free and trapped electrons were also varied as shown in figure 4, with the rate constants as for figure 1. In all cases, the free-electron percentage is shown, and the remaining percentage of trapped electrons comprises a three-to-one ratio of shallow- to deep-trapped electrons, with the total electron concentration equal to 1.00×10^{-6} M. In general, as the percentage of free electrons is increased from 50%, the plateau regions appear at progressively longer times. Also with each successive increase in the percentage of free electrons, the relative increase in the overall decay rate becomes greater.

6. Discussion

The two-level electron-detrapping model qualitatively describes the features observed experimentally. Varying the rate constant for shallow detrapping, k_2, shows dramatically the sensitivity of the model to changes in parameters (figure 2). For a value of 9×10^2 s^{-1}, k_2

would be less than k_3, so the lowest value used was 9×10^3 s^{-1}, for which only the first plateau is observed. It appears at earlier times with further increases in k_2. At 9×10^4 s^{-1}, two plateau regions are observed; however, by 9×10^6 s^{-1}, the first plateau has almost disappeared.

Since k_2 is the rate constant for the detrapping of the shallow-trapped electrons, increasing this parameter will precipitate the appearance of the first detrapping plateau. This example shows just how sensitive the model is to changes, particularly in k_2, the rate constant for shallow detrapping. In increasing k_2 from 9×10^3 s^{-1} to 9×10^5 s^{-1}, the plateau behaviour changes significantly.

Figure 3 shows the effect of varying the rate constant for deep detrapping, k_3. For low values of k_3, the second plateau region is extended for longer times, and its initial appearance is later. By 5×10^3 s^{-1}, the second plateau has almost disappeared, and by 5×10^4 s^{-1} the plateau is indistinguishable from the final decaying component of the kinetic curve. By the time k_3 has been increased to 5×10^4 s^{-1}, it has become almost equal to the shallow-detrapping rate constant, k_2 (9×10^4 s^{-1}).

Varying the relative concentrations of the species has a much more subtle effect than varying the rate constants (figure 4). The higher the concentration of shallow-trapped electrons, the earlier is the first plateau.

Rosenblatt *et al* [3] proposed that the subtle differences between F and F^+ phosphorescence in TCR MgO over many decades of time may be due to a significant number of recombinations occurring by tunnelling from nearby traps in a similar manner to donor–acceptor recombination [11]. In TCR crystals the H^- ion is the dominant electron trap controlling the phosphorescence [3].

Edel *et al* [15] had suggested that F centres themselves may act as electron traps controlling the delayed F-centre luminescence through a suggested $F^\dagger$ state. The $F^\dagger$ state produces an F^+ centre and an electron, and the free electron can recombine with an ionized F centre to produce F luminescence.

In the model developed by Rosenblatt *et al* [3], optical excitation (using a 248 nm KrF laser pulse) of an F^{+*} produces an F^* together with a hole in the valence band. Excitation of an F^{2+} centre also releases a hole into the valence band, producing an F^+ centre with an electron in the conduction band. Recombination of the F^* or the F^+ produces F-centre luminescence in both cases.

Similar behaviour of the luminescence decay curves was observed in TCR, electron- and neutron-irradiated CaO by Park *et al* [4]. It was suggested that the similarity of F^+-centre luminescence decays at both 77 and 295 K was due to either very shallow traps or tunnelling recombination.

A fundamental difference between the present experimental data (figure 1) and those of Rosenblatt *et al* [3] and Park *et al* [4] must be stressed. The latter two experiments involve the re-excitation of pre-existing defects. In the case of Rosenblatt *et al*, the defects in MgO had been introduced by thermochemical reduction, and in the case of Park *et al*, luminescence decay curves were given for TCR, electron- and neutron-irradiated CaO. It is known from previous results [22] that electrons of energy 0.48 MeV will be able to create new point defects in the lattice of Spicer sapphire (since the threshold is 0.30 MeV). The data in figure 1 originate from many individual data files, sequentially normalized to produce an overall decay curve. The possibility needs to be considered that the multiple irradiations needed to produce a single extended decay curve may create sufficient defects to modify the behaviour from that of a previously unirradiated crystal. The interaction of high-energy electrons with the lattice is well characterized by cross sections for radiolytic processes such as excitation, ionization and displacement. The concentrations of aluminium

and oxygen lattice ions are many orders of magnitude greater than those of F-type defects generated by a single pulse of irradiating electrons. We estimate that there are approximately 10^6 more lattice ions than induced F-type defects. Thus the subsequent interactions of the initial irradiating electrons will be with lattice ions rather than previously created defects. We also observe no detectable difference between the initially observed (first pulse of a new series) decay kinetics and those after a series of irradiations.

Some evidence for assigning the defect responsible for the 300 nm emission band has been presented in a previous publication [22], but given that this band has never been observed by other workers, more results are needed before the identity of the defect can be confirmed. However, the similarity of the luminescence decay behaviour for this defect to that observed in the studies of Rosenblatt *et al* [3] and Park *et al* [4] is unquestionable, suggesting that the emission arises from a very similar process.

7. Summary

Previous studies by Rosenblatt *et al* [3] and Park *et al* [4] and the present observations are all consistent with the time dependence of F-type luminescence in oxide crystals being characterized by a slow phosphorescence controlled by the thermal release of trapped electrons which recombine with defect centres. Discrete plateau features punctuate the overall luminescence decay, precluding its description by a single power law.

The present theoretical model, which involves detrapping of electrons and subsequent radiative recombination at ionized defect sites, simulates the general aspects of the experimental data. Clearly the simpler models of luminescence decay, and some of the more complex theories which have been proposed, are far from satisfactory and are unable to account for the observed experimental features. The two-level electron-detrapping model provides a physical basis for explaining some of the features of the observed luminescence decay curves. Low-temperature measurements of luminescence decay in sapphire, currently being conducted, will provide a more detailed understanding of trap depths.

Acknowledgment

The authors wish to acknowledge the support of the AINSE.

References

[1] Caulfield K J, Cooper R and Boas J F 1995 *J. Am. Ceram. Soc.* **78** 1054
[2] Williams R T, Williams J W, Turner T J and Lee K H 1979 *Phys. Rev.* B **20** 1687
[3] Rosenblatt G H, Rowe M W, Williams G P Jr, Williams R T and Chen Y 1989 *Phys. Rev.* B **39** 10 309
[4] Park J L, Chen Y, Williams G P Jr, Williams R T and Pogatshnik G J 1991 *Phys. Rev.* B **43** 11 991
[5] Randall J T and Wilkins M H F 1945 *Proc. R. Soc.* **184** 366
[6] Becquerel E 1867 *La Lumiére, ses Causes et ses Effets* (Paris: Firmin Didot)
[7] Garlick G F J and Gibson A F 1948 *Proc. Phys. Soc.* **60** 574
[8] Apple E F and Williams F E 1959 *J. Electrochem. Soc.* **106** 224
[9] Prener J S and Williams F E 1956 *Phys. Rev.* **101** 1427
[10] Williams F E 1960 *J. Phys. Chem. Solids* **12** 265
[11] Thomas D G, Hopfield J J and Augustyniak W M 1965 *Phys. Rev.* A **140** 202
[12] Jonscher A K and de Polignac A 1984 *J. Phys. C: Solid State Phys.* **17** 6493
[13] Jonscher A K 1983 *Dielectric Relaxation in Solids* (London: Chelsea Dielectrics)
[14] Jonscher A K and Li J-R 1983 *J. Phys. C: Solid State Phys.* **16** L1159
[15] Edel P, Henderson B and Romestain R 1982 *J. Phys. C: Solid State Phys.* **15** 1569
[16] Chen Y and Gonzalez R 1985 *Cryst. Lattice Defects Amorph. Mater.* **12** 149

[17] Chen Y, Gonzalez R, Schow O E and Summers G P 1983 *Phys. Rev.* B **27** 1276
[18] Jeffries B T, Gonzalez R, Chen Y and Summers G P 1982 *Phys. Rev.* B **25** 2077
[19] Swandic J R 1992 *Phys. Rev.* B **45** 622
[20] Hughes R C 1979 *Phys. Rev.* B **19** 5318
[21] Klaffky R W, Rose B H, Goland A N and Dienes G J 1980 *Phys. Rev.* B **21** 3610
[22] Caulfield K J, Cooper R and Boas J F 1993 *Phys. Rev.* B **47** 51
[23] Deuflhard P, Bader G and Nowak U 1981 *Modelling of Chemical Reaction Systems (Springer Series in Chemical Physics 18)* ed K H Ebert, P Deuflhard and W Jäger (Berlin: Springer) pp 38–54
[24] Brewer J D, Jeffries B T and Summers G P 1980 *Phys. Rev.* B **22** 4900
[25] Evans B D and Stapelbroek M 1978 *Phys. Rev.* B **18** 7089
[26] Arnold G W and Compton A D 1960 *Phys. Rev. Lett.* **4** 66